# Diffusion-controlled dissolution of a binary solid into a ternary liquid with partially-molten zone formation

By D. C. Hatton and A. W. Woods

*BP Institute for Multi-Phase Flow, University of Cambridge, Madingley Road, Cambridge CB3 0EZ, UK.*

We build a theoretical model of equilibrium dissolution of a homogeneous, solid mixture of two salts A and B, $KCl$ and $NaCl$ being used as the type example, into an aqueous solution of the two salts, with diffusive transport. We find that there are two sharp dissolution fronts, separating fluid, a partially-molten zone containing a single solid, and mixed solid. The phase change happens almost entirely at the two sharp fronts. In equilibrium, the leading front exhibits a small amount of precipitation of $NaCl$, simultaneous with complete dissolution of $KCl$. There is a unique surface in the space of far-field fluid $KCl$ concentration, far-field fluid $NaCl$ concentration, and solid composition, dividing conditions where $NaCl$ is the solid in the partially-molten zone, from conditions where $KCl$ is the solid in the partially-molten zone. The movement rates of the dissolution fronts decrease as the concentration of either salt in the far-field fluid is increased. The movement rates of the dissolution fronts increase as either far-field temperature is increased, but this effect is smaller than that of concentration. In most circumstances, the dissolution front for a given salt moves more slowly, the more of that salt is present in the original solid, although the mass dissolution rate is not greatly affected by the solid composition.

**Keywords: dissolution, melting, diffusion, conduction, salt, ice**

## 1. Introduction

In many evaporites, there are layers composed of an intimate mixture of crystals of $NaCl$ and $KCl$, and there is interest in developing physical understanding of the natural or industrial dissolution of such layers (cf. Sonnenfeld 1985; Garrett 1996; Titkov 2004).

Recently, we modelled dissolution of a single, pure solid into a three-component liquid (Hatton & Woods 2007). We focused on dissolution of $KCl$ or $NaCl$, into an aqueous solution of both salts. We showed that the dissolution rate depends on the concentrations of $KCl$ and $NaCl$ in solution. We also showed that, with a solution of a particular concentration, $KCl$ dissolves faster than $NaCl$, unless the concentration of $KCl$ in solution is close to saturation, in which case $NaCl$ dissolves faster.

When a mixed solid dissolves, the length scale over which salt can be transported diffusively will initially be short enough that any given parcel of fluid can only be affected by one solid salt, a situation equivalent to dissolution of a pure salt. We

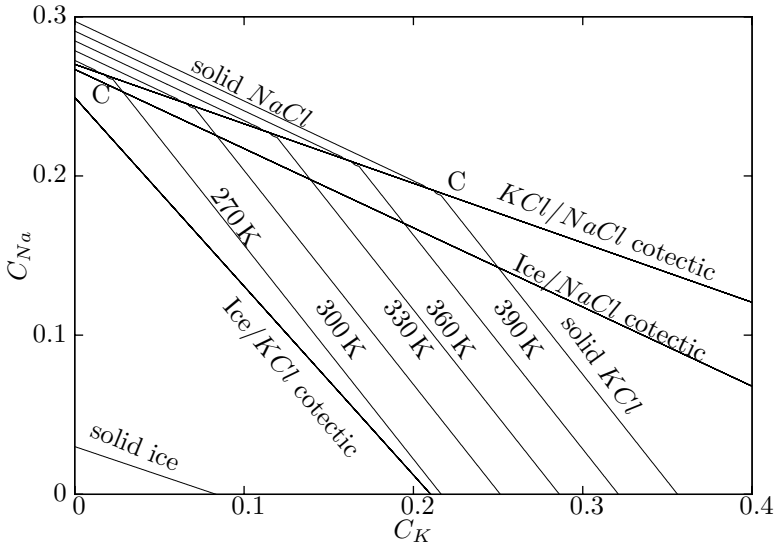


Figure 1. Constant temperature contours and cotectic lines, in ($KCl$ concentration, $NaCl$ concentration) space, in our multi-linear phase equilibrium model.

expect that the different dissolution rates of the two salts in this stage will lead to the formation of a partially-solid, two-phase zone, because the dissolution front for one salt advances more rapidly into the solid than the other. In this paper, we develop an equilibrium model of subsequent growth of the two-phase zone, in the context of diffusion-controlled mass transfer, once the diffusion lengths become long enough that not only can the fluid be affected by crystals of both salts, but the separation into individual crystals is on too small a length scale to be relevant, and the system behaves as if the solid is a homogeneous mixture. As we noted previously (Hatton & Woods 2007), the assumption that transport is diffusive may be relevant to natural dissolution of newly-formed evaporites when a lagoon floods with ocean water, and to melting of sea ice into underlying ocean water. However, we envisage that some of the physical principles we derive will carry over to situations with forced or natural convection.

## 2. Phase equilibrium model

We develop an equilibrium model (section 3). Figure 1 illustrates what we mean by "phase equilibrium." The model on which it is based states that, for aqueous solution, of salt A ($KCl$) concentration $C_A$ and salt B ($NaCl$) concentration $C_B$, to be in phase equilibrium with a solid $i \in \{A, B, I\}$ (i.e. salt A ($KCl$), salt B ($NaCl$), or ice, respectively), the temperature is

$$T = a_i C_A + b_i C_B - c_i. \tag{2.1}$$

As described in Hatton & Woods (2007), we obtained values for the nine parameters $a_i$, $b_i$, $c_i$, by fitting to empirical data gleaned from Linke (1965 (1907)) and Hall *et al.* (1988). The values are tabulated in table 1.

| Parameter | Value/ K | Parameter | Value |
|---|---|---|---|
| $a_A$ | 859.8 | $R$ | 1.09 |
| $b_A$ | 639.6 | $K_L$ | 0.140 (0.561 W/ m/ K) |
| $c_A$ | −83.9 | $K_S$ (solid $KCl$) | 0.0160 (6.95 W/ m/ K) |
| $a_B$ | 2443.2 | $K_S$ (solid $NaCl$) | 0.0209 (5.02 W/ m/ K) |
| $b_B$ | 4875.9 | $L_A$ | 229.9 kJ/ kg |
| $c_B$ | 1059.1 | $L_B$ | 17.1 kJ/ kg |
| $a_I$ | −44.0 | $l_I$ | 142 K |
| $b_I$ | −122.68 | $\rho_{SA}$ (solid $KCl$) | 1.984 t/ m$^3$ |
| $c_I$ | −273.67 | $\rho_{SB}$ (solid $NaCl$) | 2.165 t/ m$^3$ |
| | | $\rho_L$ | 1.109 t/ m$^3$ |

Table 1. *Values of parameters in our model. On the left are phase-equilibrium parameters obtained as described in the caption of figure 1 and in Hatton & Woods (2007). On the right are parameters obtained directly from the literature (Clauser & Huenges 1995; Lewis[ Peggs] 1995 (1911); Richardson 1995 (1911); Morrell 1995 (1911); Phillips 1995 (1911)*a,b*; McGlashan 1995 (1911)*b,a*; Marliacy* et al. *1998; Wheeler & Newman 2004; Ramos* et al. *2005). Salt A is KCl and salt B is NaCl. Thermal conductivities underlying $K_L$ and $K_S$ values are in brackets.*

A solution in contact with two solids is constrained by phase equilibrium to lie on the cotectic line, represented in the figure 1 by the sequence of invariant points C. Each point C relates to a particular temperature. Solution that only lies in contact with one solid is only constrained to lie on the branch of the phase-equilibrium surface relating to that solid. The solution evolves (in space) along that surface to the cotectic, as it approaches a point of contact with the second solid. This is illustrated schematically as the line $BC$ in figure 2a. Figure 2b shows this path again, with position made explicit, and information on temperature and solid fraction. Unless there is a large change in temperature between points B and C, the fluid in contact with solid $NaCl$ decreases in $NaCl$ concentration, and increases in $KCl$ concentration, as one approaches a point of contact with solid $KCl$. Therefore, $NaCl$ and $KCl$ are transported in opposite directions. This raises the possibility that, as $KCl$ dissolves at point C, $NaCl$ is precipitated. In field studies, the process in which one salt precipitates in response to dissolution of the other salt is known as "salting out" (cf. Garrett 1996).

To incorporate the restriction of salt transport in the partially-molten zone due to salting out, we set the cross-sectional area available for transport, and therefore the ratio of flux to concentration gradient, to be proportional to the liquid volume fraction. The precipitate morphology may involve complex dendritic structures, but we adopt a laterally-averaged model, to describe conservation of heat and both salts. The detailed morphology is beyond the scope of the present study.

In section 5, we present quantitative predictions from our model, and give physical explanations for them. In section 7, we highlight a few important conclusions from these results. In appendix A, we compare those predictions with a simplified, disequilibrium model, which neglects salting out. We show that salting out has only a small effect on the dissolution rate.

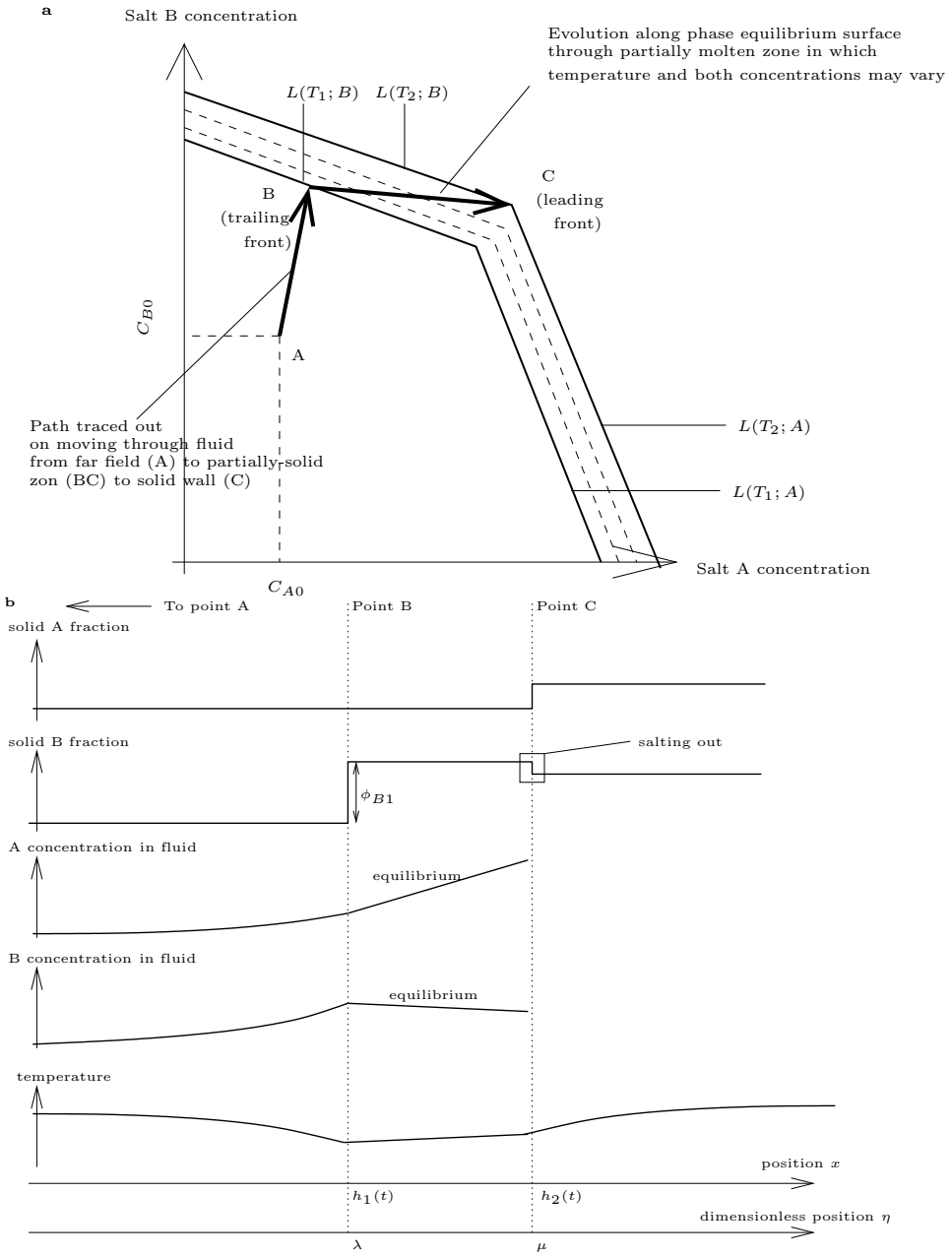


Figure 2. **a:** Schematic of path in (salt A concentration, salt B concentration) space traced out, on moving from far-field fluid (point A), past trailing front (point B), to leading front (point C). Curves $L(T_l; X)$ represent phase equilibrium curves for ternary solution of A and B and unary solid $X \in \{A, B\}$; each curve corresponds to a different temperature $T_l$. Typically solubility increases with increasing temperature, $T_2 > T_1$. **b:** Schematic illustration of solid fractions, concentrations, and temperature, as functions of position.

## 3. Physical laws

If a unit-volume, local element of the system contains a mass $m_W$ of water, $m_{AL}$ of dissolved salt A, $m_{BL}$ of dissolved salt B, $m_{AS}$ of solid salt A, and $m_{BS}$ of solid salt B, we denote the concentrations of A and B by

$$C_A = \frac{m_{AL}}{m_{AL} + m_{BL} + m_W} \tag{3.1}$$

and

$$C_B = \frac{m_{BL}}{m_{AL} + m_{BL} + m_W}. \tag{3.2}$$

Also, the solid mass fractions $\phi_A$ and $\phi_B$ are denoted

$$\phi_A = \frac{m_{AS}}{m_{AS} + m_{AL} + m_{BL} + m_{BS} + m_W}, \tag{3.3}$$

and

$$\phi_B = \frac{m_{BS}}{m_{AS} + m_{AL} + m_{BL} + m_{BS} + m_W}. \tag{3.4}$$

We use the solid mass fractions $\phi_A$ and $\phi_B$ to represent the solid volume fractions.

### (*a*) *Within the fluid region,* $x < h_1(t)$

Salt A is conserved. Therefore, the rate of change of salt A concentration matches the spatial gradient of diffusive salt A flux. The latter is given by the spatial curvature of salt A concentration:

$$D_A \frac{\partial^2 C_A}{\partial x^2} = \frac{\partial C_A}{\partial t}, \tag{3.5}$$

where $x$ is the position co-ordinate, $t$ is the time, and $D_A$ is the salt A diffusion coefficient.

Similarly for salt B:

$$D_B \frac{\partial^2 C_B}{\partial x^2} = \frac{\partial C_B}{\partial t}, \tag{3.6}$$

where $D_B$ is the salt B diffusion coefficient.

Heat is conserved. Therefore, the rate of change of temperature $T$ matches the spatial gradient of conductive heat flux:

$$\kappa_L \frac{\partial^2 T}{\partial x^2} = \frac{\partial T}{\partial t}, \tag{3.7}$$

where $\kappa_L$ is the thermal diffusivity (cf. Batchelor 1973 (1967) p. 35) of the fluid.

### (*b*) *Within the partially-molten zone,* $h_1(t) \le x < h_2(t)$

Salt A is conserved. Therefore, the rate of change of dissolved salt A content matches the spatial gradient of salt A flux. Both quantities are adjusted to allow for the possibility of a varying solid fraction:

$$D_A \frac{\partial}{\partial x}\left((1-\phi_B)\frac{\partial C_A}{\partial x}\right) = \frac{\partial}{\partial t}\left((1-\phi_B)C_A\right). \tag{3.8}$$

Salt B is conserved. Therefore, the rate of change of dissolved salt B concentration and the dissolved salt B source or sink provided by phase change match the spatial gradient of salt B flux. All three quantities are adjusted to allow for the possibility of a varying solid fraction:

$$D_B \frac{\partial}{\partial x}\left((1-\phi_B)\frac{\partial C_B}{\partial x}\right) = \frac{\partial}{\partial t}\left((1-\phi_B)C_B + \phi_B\right). \tag{3.9}$$

We have neglected the effects of variation in the partially-molten material density, $\rho_M \equiv m_{AL} + m_{BL} + m_{BS} + m_W$. We have extended this approximation to neglect the effects of the difference between the densities of the solid salts, $\rho_{SA}$ and $\rho_{SB}$, and $\rho_M$; hence, we define a universal density by a weighted geometric average $\rho = ((\rho_{SA}\rho_{SB})^{1/2}\rho_L)^{1/2}$, where $\rho_L$ is the density of the liquid. Water is then automatically conserved by conserving both salts. During development of the single-solid model (Hatton & Woods 2007), we explored the effects of the density difference between solid and liquid. The density difference introduced a small, uniform velocity field, directed away from the solid, which reduced the dissolution rates by a factor of 1.7–1.8 (approximately the ratio of solid density to liquid density), without changing their functional dependences on the far-field conditions. An analogous effect will occur herein, but we neglect it for simplicity.

Heat is conserved. Therefore, the rate of change of temperature and the sensible heat source or sink provided by the latent heat associated with phase change of salt B match the spatial gradient of heat flux:

$$k_M \frac{\partial^2 T}{\partial x^2} = \rho H_M \frac{\partial T}{\partial t} - L_B \rho \frac{\partial \phi_B}{\partial t}, \tag{3.10}$$

where $k_M$ is the thermal conductivity of the partially-molten material and $L_B$ is the specific latent heat of dissolution of solid salt B. We estimate $k_M$ by considering conduction through liquid (thermal conductivity $k_L$) and solid salt B (thermal conductivity $k_{SB}$) in parallel (cf. Greitzer *et al.* 2006), with an estimated value $\phi_{B\infty}/2$ of the typical solid fraction in the partially-molten zone:

$$k_M \approx \frac{\phi_{B\infty}}{2} k_{SB} + \left(1 - \frac{\phi_{B\infty}}{2}\right) k_L,$$

where $\phi_{A\infty} = 1 - \phi_{B\infty}$ is the salt A fraction, and $\phi_{B\infty}$ the salt B fraction, in the undisturbed solid. $H_M$ is the specific heat capacity of the partially molten material, which we estimate in a similar way, from the specific heat capacities $H_{SB}$ of solid salt B and $H_L$ of liquid:

$$H_M \approx \frac{\phi_{B\infty}}{2} H_{SB} + \left(1 - \frac{\phi_{B\infty}}{2}\right) H_L.$$

Later, it will be convenient to think in terms of the thermal diffusivity of the partially-molten zone:

$$\kappa_M = \frac{k_M}{\rho H_M}.$$

Contact with solid salt B forces the liquid to be on the solid-B branch of the phase equilibrium surface:

$$T = a_B C_A + b_B C_B - c_B. \tag{3.11}$$

### (*c*) *Within the solid region, $x \geq h_2(t)$*

Heat is conserved. Therefore, the rate of change of temperature matches the spatial gradient of heat flux:

$$\kappa_S \frac{\partial^2 T}{\partial x^2} = \frac{\partial T}{\partial t}, \tag{3.12}$$

where $\kappa_S$ is the thermal diffusivity of the solid. $\kappa_S$ is constructed from the thermal properties of individual solids in the same way that $\kappa_M$ is constructed from the thermal properties of solid salt B and liquid (section b): from a thermal conductivity

$$k_S = (1 - \phi_{B\infty}) k_{SA} + \phi_{B\infty} k_{SB},$$

and a specific heat capacity

$$H_S = (1 - \phi_{B\infty}) H_{SA} + \phi_{B\infty} H_{SB},$$

where $k_{SA}$ and $H_{SA}$ are the thermal conductivity and specific heat capacity of solid salt A. The usual formula

$$\kappa_S = \frac{k_S}{\rho H_S}$$

applies.

### (*d*) *At the trailing boundary, $x = h_1(t)$*

Salt A is conserved. Therefore, the difference in salt A flux (i.e. in the product of porosity and the spatial gradient of salt A concentration) across the boundary matches the additional flux of salt A associated with movement of the boundary. The additional flux arises because the total mass fraction of salt A is, in general, different on each side of the moving boundary:

$$\begin{aligned} D_A \left( \left. \frac{\partial C_A}{\partial x} \right|_{x=h_1(t)-} - \left(1 - \left. \phi_B \right|_{x=h_1(t)+}\right) \left. \frac{\partial C_A}{\partial x} \right|_{x=h_1(t)+} \right) \\ = h_1'(t) \left( \left(1 - \left. \phi_B \right|_{x=h_1(t)+}\right) \left. C_A \right|_{x=h_1(t)+} - \left. C_A \right|_{x=h_1(t)-} \right). \end{aligned} \tag{3.13}$$

Salt B is conserved. By analogy with conservation of salt A, this leads to the relation:

$$\begin{aligned} D_B \left( \left. \frac{\partial C_B}{\partial x} \right|_{x=h_1(t)-} - \left(1 - \left. \phi_B \right|_{x=h_1(t)+}\right) \left. \frac{\partial C_B}{\partial x} \right|_{x=h_1(t)+} \right) \\ = h_1'(t) \left( \left(1 - \left. \phi_B \right|_{x=h_1(t)+}\right) \left. C_B \right|_{x=h_1(t)+} + \left. \phi_B \right|_{x=h_1(t)+} - \left. C_B \right|_{x=h_1(t)-} \right). \end{aligned} \tag{3.14}$$

Heat is conserved. Therefore, the difference in heat flux (i.e. in the spatial gradient of temperature, adjusted for the different thermal diffusivities of fluid region and partially-molten zone) across the boundary matches the sensible heat source or sink, provided by the latent heat associated with phase change of salt B as the boundary moves:

$$k_L \left. \frac{\partial T}{\partial x} \right|_{x=h_1(t)-} - k_M \left. \frac{\partial T}{\partial x} \right|_{x=h_1(t)+} = -h_1'(t) L_B \rho \left. \phi_B \right|_{x=h_1(t)+}, \tag{3.15}$$

where $H_L$ is the specific heat capacity of the liquid.

Temperature is continuous (cf. Glass *et al.* 1991):

$$T|_{x=h_1(t)-} = T|_{x=h_1(t)+}\,. \tag{3.16}$$

Salt concentrations are continuous (cf. Glass *et al.* 1991):

$$C_A|_{x=h_1(t)-} = C_A|_{x=h_1(t)+}\,. \tag{3.17}$$

$$C_B|_{x=h_1(t)-} = C_B|_{x=h_1(t)+}\,. \tag{3.18}$$

The fluid immediately to the left is in phase equilibrium with solid salt B:

$$T|_{x=h_1(t)-} = a_B\, C_A|_{x=h_1(t)-} + b_B\, C_B|_{x=h_1(t)-} - c_B. \tag{3.19}$$

($e$) *At the leading boundary, $x = h_2\,(t)$*

Salt A is conserved. Therefore, the diffusive salt A flux immediately to the left matches the flux of salt A associated with the phase change:

$$(1-\phi_B|_{x=h_2(t)-})D_A\,\left.\frac{\partial C_A}{\partial x}\right|_{x=h_2(t)-} = h_2'\,(t)\left(\phi_A|_{x=h_2(t)+} - \left(1-\,\phi_B|_{x=h_2(t)-}\right)\,C_A|_{x=h_2(t)-}\right). \tag{3.20}$$

Similarly, for salt B:

$$(1-\phi_B|_{x=h_2(t)-})D_B\,\left.\frac{\partial C_B}{\partial x}\right|_{x=h_2(t)-} = h_2'\,(t)\left(\phi_B|_{x=h_2(t)+} - \,\phi_B|_{x=h_2(t)-} - \left(1-\,\phi_B|_{x=h_2(t)-}\right)\,C_B|_{x=h_2(t)-}\right). \tag{3.21}$$

Heat is conserved. Therefore, the difference in heat flux across the boundary matches the sensible heat source or sink provided by the latent heat associated with precipitation or dissolution of salts as the boundary moves:

$$k_M\,\left.\frac{\partial T}{\partial x}\right|_{x=h_2(t)-} - k_S\,\left.\frac{\partial T}{\partial x}\right|_{x=h_2(t)+} = h_2'\,(t)\left(-L_A\rho\,\phi_A|_{x=h_2(t)+} + L_B\rho\left(\phi_B|_{x=h_2(t)-} - \,\phi_B|_{x=h_2(t)+}\right)\right). \tag{3.22}$$

where $L_A$ is the specific latent heat of dissolution for salt A.

Temperature is continuous:

$$T|_{x=h_2(t)-} = T|_{x=h_2(t)+}\,. \tag{3.23}$$

The fluid immediately to the left is in phase equilibrium with both solid salts (i.e. on the cotectic):

$$T|_{x=h_2(t)-} = a_A\, C_A|_{x=h_2(t)-} + b_A\, C_B|_{x=h_2(t)-} - c_A. \tag{3.24}$$

$$T|_{x=h_2(t)-} = a_B\, C_A|_{x=h_2(t)-} + b_B\, C_B|_{x=h_2(t)-} - c_B. \tag{3.25}$$

## 4. Self-similar solutions

Equations 3.5–3.12 admit self-similar solutions, i.e. the concentrations $C_A$ and $C_B$, solid fractions $\phi_A$ and $\phi_B$, and temperature $T$ depend on position $x$ and time $t$ only through a similarity variable $\eta = x/\sqrt{2\sqrt{D_A D_B}t}$ (cf. Carslaw & Jaegar 1959 (1946); Woods 1992). This converts time-dependent boundary positions to constant positions in $\eta$ space, $\lambda = h_1(t)/\sqrt{2\sqrt{D_A D_B}t}$ and $\mu = h_2(t)/\sqrt{2\sqrt{D_A D_B}}$. $\lambda$ and $\mu$ are proportional to the product of front velocity and the square root of time, so they also serve as rate constants. Self-similarity also transforms partial differential equations to ordinary differential equations.

### (*a*) *The fluid region, $\eta < \lambda$*

The self-similar solutions of equations 3.5–3.7 are (Hatton & Woods 2007):

$$C_A = C_{A0} + \Delta C_{A0} G\left(\frac{\eta}{R}\right), \tag{4.1}$$

$$C_B = C_{B0} + \Delta C_{B0} G\left(R\eta\right), \tag{4.2}$$

and

$$T = T_f + \Delta T_0 G\left(K_L \eta\right), \tag{4.3}$$

where the error function $G(z)$ is defined, in terms of the normalized Gaussian

$$g(u) = \frac{\exp\left(-u^2/2\right)}{\sqrt{2\pi}}, \tag{4.4}$$

as

$$G(z) = \int_{u=-\infty}^{z} g(u)\,\mathrm{d}u. \tag{4.5}$$

$R = (D_A/D_B)^{1/4}$ is the ratio of fourth roots of the solutal diffusivities for the two salts, and $K_L = \sqrt{\sqrt{D_A D_B}/\kappa_L}$ is the inverse square root of the Lewis number (cf. Josberger & Martin 1981). $C_{A0}$, $C_{B0}$, and $T_f$ are the known far-field fluid concentrations and temperature. $\Delta C_{A0}$, $\Delta C_{B0}$, and $\Delta T_0$ are parameters indicating the amplitude of concentration and temperature variation, to be determined from equations 3.13–3.15. The resulting values are stated in appendix C.

### (*b*) *The solid region, $\eta \geq \mu$*

The self-similar solution of equation 3.12 is (Hatton & Woods 2007):

$$T = T_s + \Delta T_2 \left(G\left(K_S \eta\right) - 1\right). \tag{4.6}$$

$K_S = \sqrt{\sqrt{D_A D_B}/\kappa_S}$ is the solid equivalent of $K_L$. $T_s$ is the known far-field solid temperature. $\Delta T_2$ is a parameter indicating the amplitude of temperature variation, to be determined from equation 3.23. The resulting value is stated in appendix C.

### (c) *The partially-molten zone, $\lambda \leq \eta < \mu$*

Self-similarity reduces equation 3.8 to

$$(1-\phi_B)\frac{\mathrm{d}^2 C_A}{\mathrm{d}\eta^2} - \frac{\mathrm{d}\phi_B}{\mathrm{d}\eta}\frac{\mathrm{d}C_A}{\mathrm{d}\eta} = -\frac{\eta}{R^2}\left((1-\phi_B)\frac{\mathrm{d}C_A}{\mathrm{d}\eta} - \frac{\mathrm{d}\phi_B}{\mathrm{d}\eta}C_A\right), \tag{4.7}$$

equation 3.9 to

$$(1-\phi_B)\frac{\mathrm{d}^2 C_B}{\mathrm{d}\eta^2} - \frac{\mathrm{d}\phi_B}{\mathrm{d}\eta}\frac{\mathrm{d}C_B}{\mathrm{d}\eta} = -R^2\eta\left((1-\phi_B)\frac{\mathrm{d}C_B}{\mathrm{d}\eta} + \frac{\mathrm{d}\phi_B}{\mathrm{d}\eta}(1-C_B)\right), \tag{4.8}$$

and equation 3.10 to

$$\frac{\mathrm{d}^2 T}{\mathrm{d}\eta^2} = -K_M^2\eta\left(\frac{\mathrm{d}T}{\mathrm{d}\eta} - \frac{L_B}{H_M}\frac{\mathrm{d}\phi_B}{\mathrm{d}\eta}\right), \tag{4.9}$$

where $K_M = \sqrt{\sqrt{D_A D_B}/\kappa_M}$ is the partially-molten zone equivalent of $K_L$.

We use the approximation $R \approx 1$. This is not very restrictive: most common ions have diffusivities in water within a factor of 2 either side of $1.6 \times 10^{-9}\,\mathrm{m}^2/\mathrm{s}$ (Vanýsek 2001). We add the product of $a_B$ and equation 4.7 to the product of $b_B$ and equation 4.8, and substitute from equation 3.11, to obtain

$$\eta\frac{\mathrm{d}\phi_B}{\mathrm{d}\eta} = \frac{1}{T_f + c_B - b_B}\left((1-\phi_B)\frac{\mathrm{d}^2 T}{\mathrm{d}\eta^2} - \frac{\mathrm{d}\phi_B}{\mathrm{d}\eta}\frac{\mathrm{d}T}{\mathrm{d}\eta} - \eta\left(\frac{\mathrm{d}\phi_B}{\mathrm{d}\eta}(T-T_f) - (1-\phi_B)\frac{\mathrm{d}T}{\mathrm{d}\eta}\right)\right). \tag{4.10}$$

We take advantage of the fact that, whether salt B is $NaCl$ or $KCl$, $b_B$, the rate at which solid-B phase equilibrium temperature varies with dissolved salt B concentration, is several thousand Kelvin or several hundred Kelvin respectively (table 1,) hence the denominator $T_f + c_B - b_B \approx -b_B$. Temperature varies on a scale, in $\eta$ space, of order $1/K_M$, so that, if the total temperature variation in the system is $\Theta$, then $\mathrm{d}T/\mathrm{d}\eta$ is of order $K_M\Theta$ and $\mathrm{d}^2T/\mathrm{d}\eta^2$ is of order $K_M^2\Theta$. We do not consider systems with temperature variations of more than a few tens of Kelvin, and $K_M < 1$, so neither derivative is nearly as large as $b_B$. The dimensionless multiplier $(1-\phi_B)$ is necessarily of order 1 or smaller. We deduce that the right-hand side of equation 4.10 is of the order of the small parameter $K_M\Theta/b_B$, and we can use a perturbation expansion with this quantity as expansion parameter to exclude the right-hand side of equation 4.10 from leading-order consideration. The expansion parameter represents the gradient, in $\eta$ space, of phase-equilibrium salt B concentration, associated with the temperature gradient. Hence, to leading order, we can simplify figure 2a to a version that is isothermal for phase-equilibrium purposes (figure 3). In its zeroth order, the perturbation expansion gives

$$\frac{\mathrm{d}\phi_B}{\mathrm{d}\eta} = 0. \tag{4.11}$$

We call this constant solid fraction

$$\phi_B = \phi_{B1} \tag{4.12}$$

(cf. figure 2b).

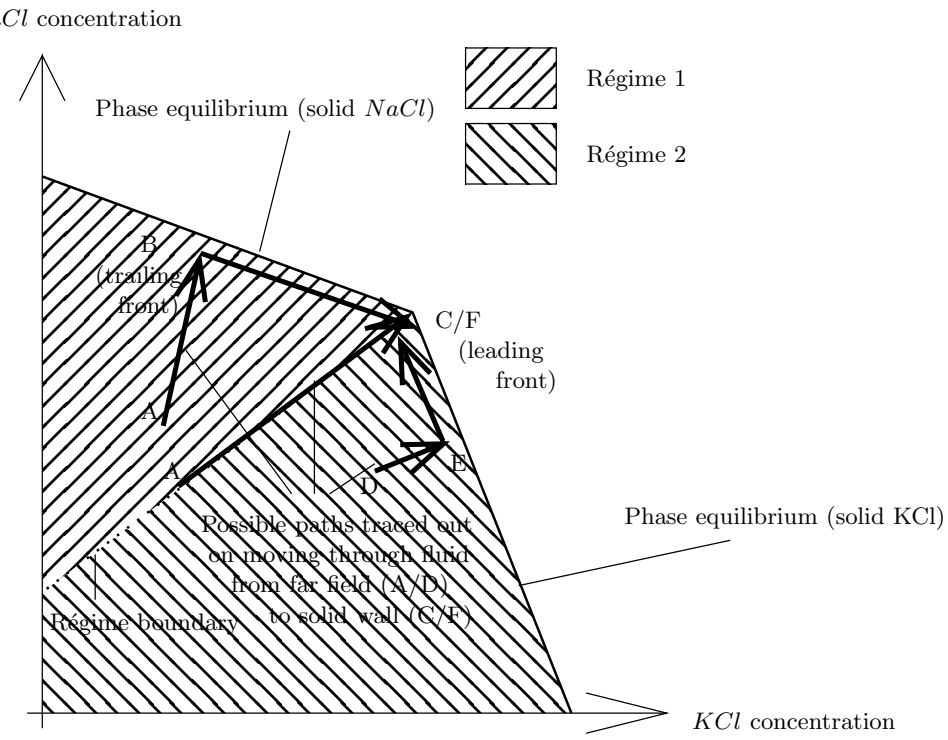


Figure 3. Schematic of path in (salt A concentration, salt B concentration) space traced out, on moving from far-field fluid (point A), past trailing front (point B), to leading front (point C), with effect of temperature on phase-equilibrium concentration neglected.

Substituting from equation 4.11 into equation 4.9, we find

$$\frac{\mathrm{d}^2 T}{\mathrm{d}\eta^2} = -K_M^2 \eta \frac{\mathrm{d}T}{\mathrm{d}\eta} \tag{4.13}$$

for $\lambda \leq \eta < \mu$, and so

$$T = T_1 + \Delta T_1 G\left(K_M \eta\right). \tag{4.14}$$

Similarly, from equations 4.11 and 4.7,

$$\frac{\mathrm{d}^2 C_A}{\mathrm{d}\eta^2} = -\eta \frac{\mathrm{d}C_A}{\mathrm{d}\eta} \tag{4.15}$$

for $\lambda \leq \eta < \mu$, and so

$$C_A = C_{A1} + \Delta C_{A1} G\left(\eta\right). \tag{4.16}$$

Similarly, from equations 4.11 and 4.8, once more using $R \approx 1$,

$$\frac{\mathrm{d}^2 C_B}{\mathrm{d}\eta^2} = -\eta \frac{\mathrm{d}C_B}{\mathrm{d}\eta} \tag{4.17}$$

for $\lambda \leq \eta < \mu$, and so

$$C_B = C_{B1} + \Delta C_{B1} G\left(\eta\right). \tag{4.18}$$

To summarize, within the partially-molten zone, the solid fraction is constant. In addition, all three "substances" (salt A, salt B, and heat) are transported independently, i,e. the concentrations of both salts in the fluid, and the temperature, vary as error functions on their respective diffusive length scales. We have introduced parameters $\phi_{B1}$, $T_1$, $\Delta T_1$, $C_{A1}$, $\Delta C_{A1}$, $C_{B1}$, and $\Delta C_{B1}$, representing the solid fraction, the baseline temperature and concentrations, and the amplitudes of temperature and concentration variation. These can be determined using equations 3.16–3.22, 3.24, and 3.25. The values are stated in appendix C.

In figure 9, we check a posteriori that the expansion parameter is small enough to justify the perturbation expansion. In appendix B, we consider the next order of the expansion.

## 5. Results

We will now discuss quantitative predictions of the model. Specifically, we analyse the system where the salts are $KCl$ and $NaCl$. Values for material properties of the system, to be inserted into the equations, are tabulated in table 1.

Figure 3 is a schematic illustrating that concentration space divides into two regions. In régime 1 (e.g. far-field composition A,) the fluid meets the solid-$NaCl$ phase equilibrium surface at the trailing front (B,) then evolves in space along that surface in a partially-molten zone containing solid $NaCl$ to the cotectic (C.) This is described by a version of our model, in which $KCl$ is salt A and $NaCl$ is salt B. In régime 2 (e.g. far-field composition D,) the fluid meets the solid-$KCl$ phase equilibrium surface at the trailing front (E,) then evolves in space along that surface in a partially-molten zone containing solid $KCl$ to the cotectic (C.) This is described by a version of our model in which $KCl$ is re-labelled "salt B" and $NaCl$ is re-labelled "salt A." Where the far-field fluid is on the régime boundary (e.g. far-field composition F) the fluid approaches the cotectic (C) from a position of under-saturation in both salts, and there is no partially-molten zone, so that the two phase-change fronts travel together, $\lambda = \mu$. This allows the régime boundary to be readily identified. In figure 4, we plot the predicted locus, in (far-field fluid $KCl$ concentration $C_{K0}$, far-field fluid $NaCl$ concentration $C_{Na0}$, far-field solid composition $\phi_{B\infty}$) space, of such conditions. Figure 4 can be interpreted as a régime diagram, specifying which salt will be solid in the partially-molten zone for given far-field conditions. The position of the boundary is independent of which version of the model is used to search for the $\lambda = \mu$ contour, i.e. there is always a unique answer to the question of which salt remains solid in the partially-molten zone. In the rest of this section, we concentrate on the régime where the solid in the partially-molten zone (salt B) is $NaCl$.

In all the circumstances we have studied, $\phi_{Na1} > \phi_{Na\infty}$, i.e. salting-out ($NaCl$ precipitation at the leading front) occurs.

In figure 5, we plot the predicted dimensionless rate constants $\lambda$ for movement of the trailing (liquid/partially-molten) interface and $\mu$ for movement of the leading (partially-molten/solid) interface, as functions of the $NaCl$ concentration $C_{Na0}$ in the far-field fluid, for several solid compositions.

The dissolution rates decrease with increasing $C_{Na0}$, as the $NaCl$ concentration contrast between far-field fluid and partially molten zone decreases, and therefore the $NaCl$ concentration gradients and fluxes decrease.

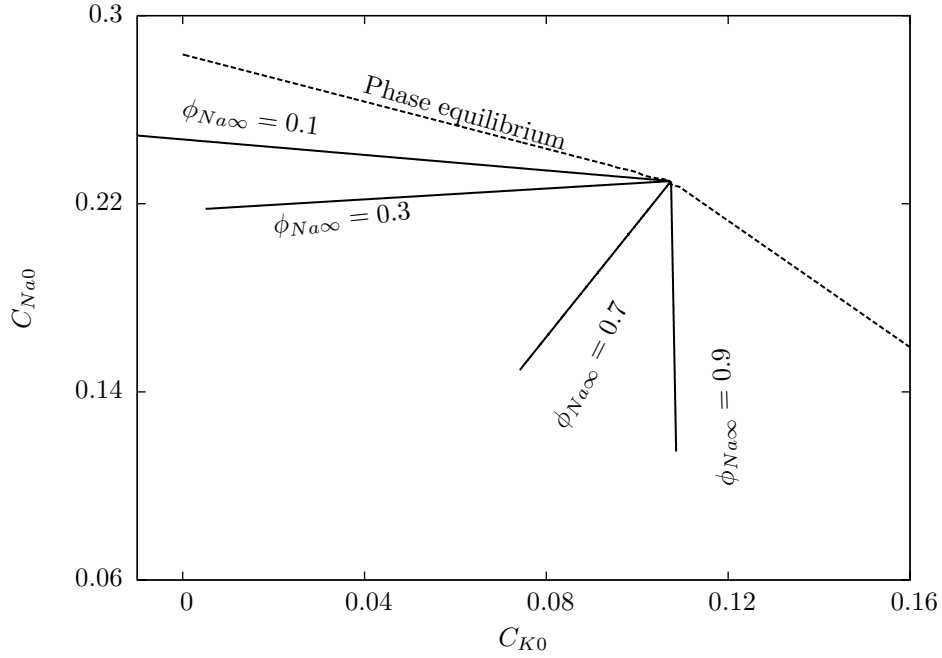


Figure 4. Predicted locus, in (far-field fluid $KCl$ concentration, far-field fluid $NaCl$ concentration, far-field solid composition) space, of conditions where the two fronts travel together, $\lambda = \mu$, and there is no partially-molten zone. Far-field fluid temperature $T_f = 50\,^{\circ}\mathrm{C}$. Far-field solid temperature $T_s = 50\,^{\circ}\mathrm{C}$.

Usually, the more of one salt is present in the far-field solid, the more slowly that salt dissolves. This is because the *mass* dissolution rate of a given salt is proportional to the product of the relevant dissolution rate parameter and the fraction of the far-field solid that is composed of that salt. Thus, the greater the fraction of the far-field solid that is composed of a particular salt, the lower the dissolution rate parameter that can be sustained by a given diffusive flux of that salt.

However, this principle breaks down at high far-field fluid $NaCl$ concentrations. At $C_{Na0} \approx 0.27$, the trailing-front velocity curves for different solid compositions cross, and for $C_{Na0} \gtrsim 0.27$, the $NaCl$ dissolution rate (trailing front velocity) increases with increasing $NaCl$ content in the far-field solid. This is possible because here, $NaCl$ dissolved at the trailing front is mostly transported towards the leading front to be re-precipitated, not towards the far-field fluid. As the $NaCl$ content of the far-field solid increases, the $KCl$ dissolution rate (leading front velocity) increases, both because of increasing $KCl$ concentration gradient in the fluid in the partially-molten zone and because of decreasing $KCl$ content in the far-field solid. Therefore, there is an increasing demand for $NaCl$ to supply re-precipitation.

Figure 5 does not include cases where the undisturbed solid is a single, pure salt, $\phi_{Na\infty} \in \{0, 1\}$. We discuss these cases separately, in section 6.

In figure 6, we plot the predicted dimensionless rate constants $\lambda$ and $\mu$, for movement of the trailing and leading interfaces, respectively, as functions of the $NaCl$ concentration $C_{Na0}$ in the far-field fluid, for several far-field fluid $KCl$ con-

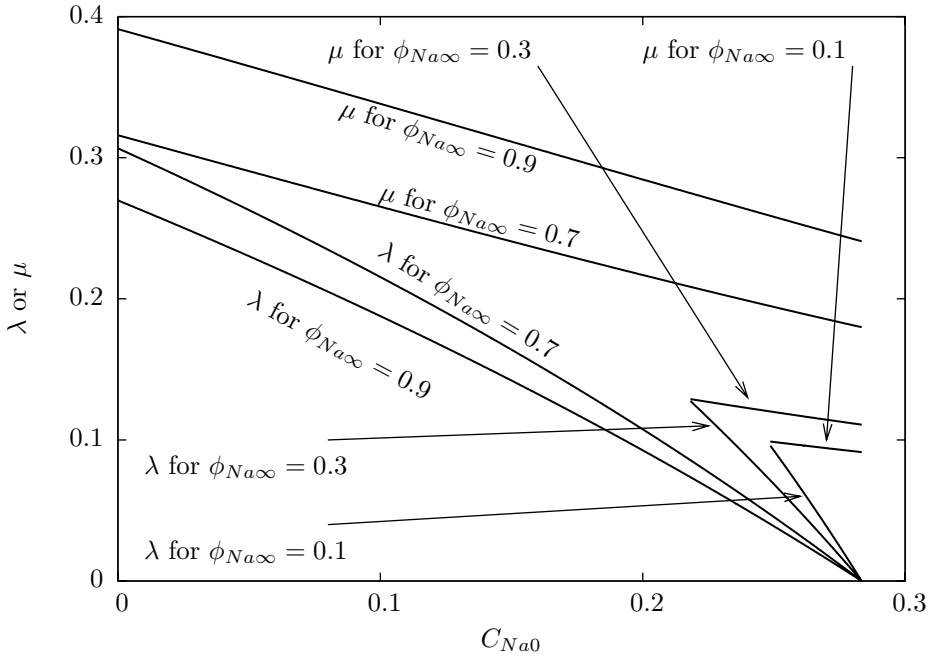


Figure 5. Predicted dimensionless rate constants $\lambda$ and $\mu$, for movement of trailing and leading interfaces, respectively, as functions of $NaCl$ concentration $C_{Na0}$ in far-field fluid. Far-field fluid contains no $KCl$, $C_{K0} = 0$. Far-field fluid temperature $T_f = 50\,^{\circ}\mathrm{C}$. Far-field solid temperature $T_s = 50\,^{\circ}\mathrm{C}$. Eight curves plotted, corresponding to the two dimensionless rate constants for each of the far-field solid compositions: $\phi_{K\infty} = 0.9$, $\phi_{Na\infty} = 0.1$; $\phi_{K\infty} = 0.7$, $\phi_{Na\infty} = 0.3$; $\phi_{K\infty} = 0.3$, $\phi_{Na\infty} = 0.7$; and $\phi_{K\infty} = 0.1$, $\phi_{Na\infty} = 0.9$.

centrations. Adding $KCl$ to the far-field fluid, like adding $NaCl$ to the far-field fluid, suppresses the dissolution rates. The reasons are analogous.

In figure 7, we plot the predicted dimensionless rate constants $\lambda$ and $\mu$, for movement of the trailing and leading interfaces, respectively, as functions of the $NaCl$ concentration $C_{Na0}$ in the far-field fluid, for several far-field fluid temperatures.

The effect of far-field fluid temperature is smaller than that of far-field fluid composition. The former relates to increased interface temperature increasing the saturation concentrations that pertain in the partially molten zone. This in turn increases the concentration gradients and fluxes between here and the far-field fluid. As for pure solids, this shift in saturation concentration is kept small by the large liquidus gradients. The curves for the leading ($KCl$ dissolution) front are very similar to those for dissolution of pure $KCl$, and the curves for the trailing ($NaCl$ dissolution) front are very similar to those for dissolution of pure $NaCl$. We explained (Hatton & Woods 2007) how the different liquidus characteristics for the two solids ensured that pure $KCl$ would dissolve faster than pure $NaCl$, except where the far-field fluid was very concentrated in $KCl$. Solid $KCl$ requires either a lower interface temperature or a higher interface concentration than solid $NaCl$ to maintain phase equilibrium. Therefore, more salt is transported away and/or more heat is available to provide latent heat for $KCl$ dissolution than for $NaCl$.

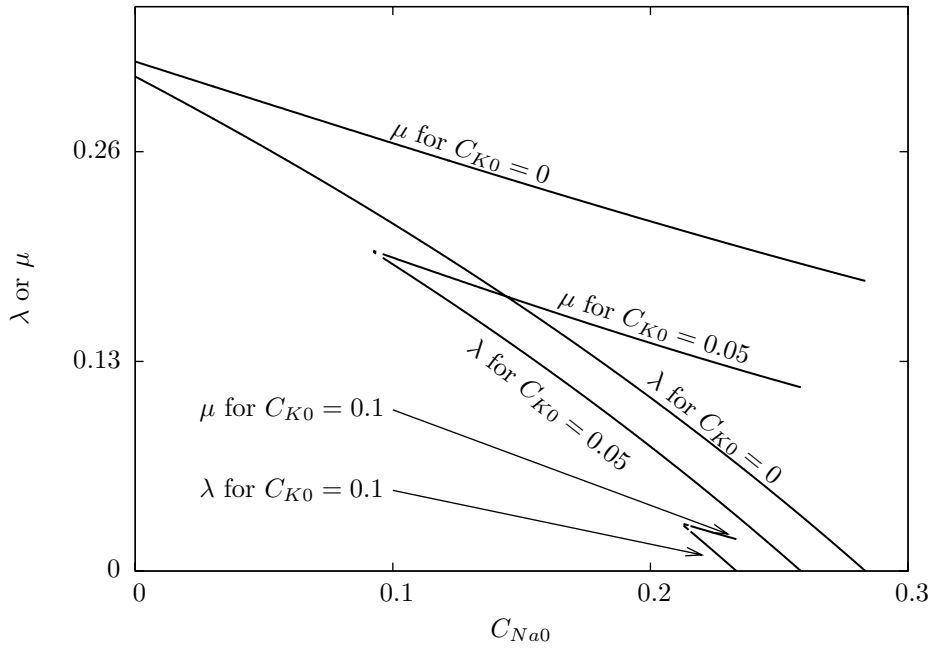


Figure 6. Predicted dimensionless rate constants $\lambda$ and $\mu$, for movement of trailing and leading interfaces, respectively, as functions of $NaCl$ concentration $C_{Na0}$ in far-field fluid. Far-field fluid temperature $T_f = 50\,^{\circ}$C. Composition of far-field solid is $\phi_{K\infty} = 0.3$, $\phi_{Na\infty} = 0.7$. Far-field solid temperature $T_s = 50\,^{\circ}$C. Six curves plotted, corresponding to the two dimensionless rate constants for each of the far-field fluid $KCl$ concentrations $C_{K0} = 0$, $C_{K0} = 0.05$, and $C_{K0} = 0.1$.

The predictions of dissolution rates in a binary solid shown in figure 7 represent an extension of this principle. The range of far-field temperatures we have imposed is larger than is geophysically realistic. Therefore, given that our imposed temperature variation has only minor effects, the temperature variations encountered in nature will have even smaller effects.

Figure 7 also includes results of numerical calculations (cf. appendix D), which illustrate what happens if one uses neither the $R \approx 1$ (equal solutal diffusivities for the two salts) approximation nor the large-$b_B$ perturbation expansion (compare symbols $\times$ and $+$ with curves generated from earlier analytic solutions). Because the solutal diffusivity for $KCl$ is slightly higher than $\sqrt{D_A D_B}$, taking account of the diffusivity difference $R \neq 1$ enhances the $KCl$ dissolution rate (symbols $\times$, figure 7). Similarly, because the solutal diffusivity for $NaCl$ is slightly lower than $\sqrt{D_A D_B}$, taking account of the diffusivity difference usually reduces the $NaCl$ dissolution rate (symbols $+$, figure 7).

As an interesting aside, in figure 8, we examine what happens to the results in figure 7 if we artificially increase the thermal conductivity $k_M$ of the partially-molten zone by a factor of 2. Doubling the thermal conductivity of partially-molten material has made little difference either to the width of the partially-molten zone or to the dissolution rates of individual solids. This is unsurprising, given that, as

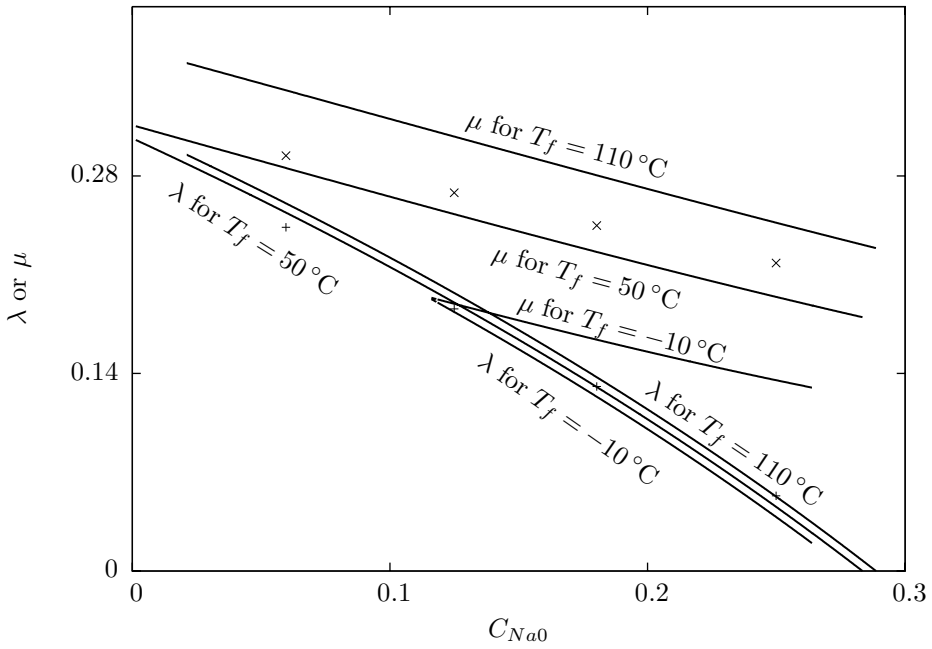


Figure 7. Predicted dimensionless rate constants $\lambda$ and $\mu$, for movement of trailing and leading interfaces, respectively, as functions of $NaCl$ concentration $C_{Na0}$ in far-field fluid. Far-field fluid contains no $KCl$, $C_{K0} = 0$. Composition of far-field solid is $\phi_{K\infty} = 0.3$, $\phi_{Na\infty} = 0.7$. Far-field solid temperature $T_s = 50\,^\circ$C. Six curves plotted, corresponding to the two dimensionless rate constants for each of the far-field fluid temperatures $T_f = -10\,^\circ$C, $T_f = 50\,^\circ$C, and $T_f = 110\,^\circ$C. Crosses represent numerical results for $T_f = 50\,^\circ$C, based on Euler solution (cf. Arfken 1985 pp. 491–492) of equations 4.7–4.9, with shooting (cf. Press *et al.* 1992 (1986) pp. 745–747) by simulated annealing (cf. MacKay 2003 p. 392) to obtain correct boundary conditions for far-field conditions (cf. appendix D). Numerical method uses neither $R \approx 1$ approximation nor large-$b_B$ perturbation expansion.

discussed above, the system behaves to leading order as if the partially-molten zone is isothermal.

Finally, we assess the validity of the perturbation expansion. In figure 9 we plot its predicted largest value, as a function of the $NaCl$ concentration $C_{Na0}$ in the far-field fluid, for several far-field fluid temperatures. The expansion parameter is always small compared with unity, as required for the expansion to be valid.

## 6. Application to dissolution of a pure solid

We can apply the model in this paper to dissolution of a pure salt (say $KCl$). When we discussed this problem before (Hatton & Woods 2007), we neglected the possibility of precipitation of a second salt (say $NaCl$) from the melt, and of formation of a partially-molten zone. Usually, the fluid remained everywhere undersaturated in $NaCl$, and we found solutions in which the only phase change was dissolution of $KCl$, which were consistent with all the physical principles discussed

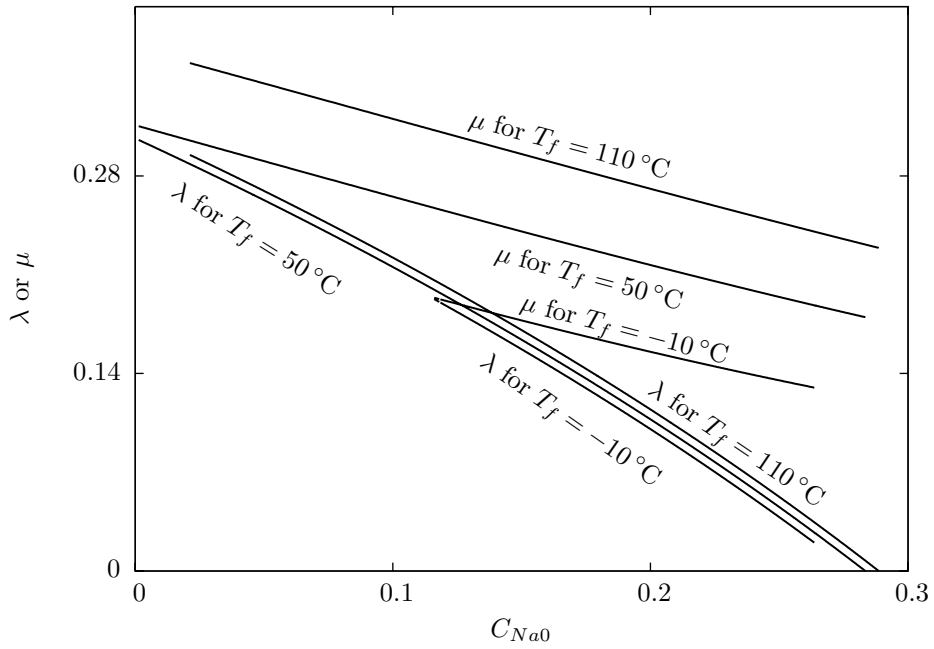


Figure 8. Predicted dimensionless rate constants $\lambda$ and $\mu$, for movement of trailing and leading interfaces, respectively, as functions of $NaCl$ concentration $C_{Na0}$ in far-field fluid. Far-field fluid contains no $KCl$, $C_{K0} = 0$. Composition of far-field solid is $\phi_{K\infty} = 0.3$, $\phi_{Na\infty} = 0.7$. Far-field solid temperature $T_s = 50\,°\mathrm{C}$. Six curves plotted, corresponding to the two dimensionless rate constants for each of the far-field fluid temperatures $T_f = -10\,°\mathrm{C}$, $T_f = 50\,°\mathrm{C}$, and $T_f = 110\,°\mathrm{C}$. Thermal conductivity of partially-molten zone artificially increased by factor of 2.

in the present paper (régime 2, figure 10a). In that case, line A–B illustrates the path followed by the solution in concentration space as the solid dissolves. This is illustrated again with position made explicit in figure 10b. However, if the far field fluid is almost saturated in $NaCl$ and the solid is composed of $KCl$ (régime 1, figure 10a,) salting out, as shown by line C–D–E in figure 10a, may occur. This is illustrated again with position made explicit in figure 10c. The new model developed in this paper, which allows for salting out, can be applied to describe this situation.

In figure 11, we present a calculation illustrating the far-field conditions $(C_{K0}, C_{Na0})$ for which $\lambda = \mu$ and hence which correspond to the limiting concentration for which salting out can occur. In the regions between this locus of far-field conditions and the phase equilibrium curves, labelled as "$NaCl$ PMZ" and "$KCl$ PMZ", salting out can occur for solid $KCl$ or solid $NaCl$ respectively. The region labelled "no PMZ" corresponds to the case in which there is no salting out.

In the region labelled "$NaCl$ PMZ", salting out precipitation produces a partially-molten zone containing solid $NaCl$, trailing the undissolved pure $KCl$ solid. In the region labelled "$KCl$ PMZ", salting out precipitation produces a partially-molten zone containing solid $KCl$, trailing the undissolved pure $NaCl$ solid.

In figure 12, we present some predictions of the model in this paper for the

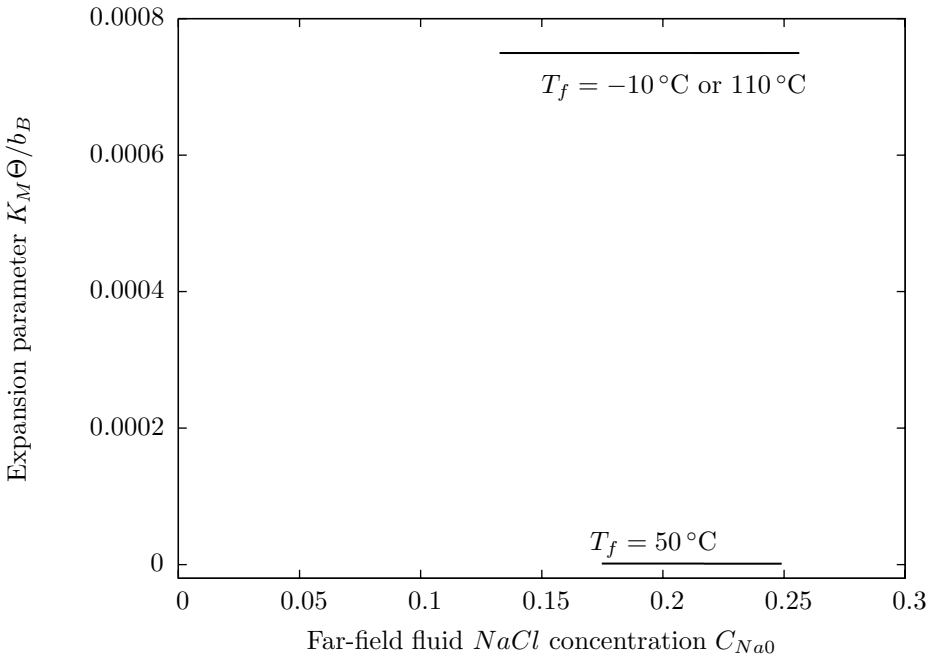


Figure 9. Predicted expansion parameter value $K_M\Theta/b_B$, as function of $NaCl$ concentration $C_{Na0}$ in the far-field fluid. Far-field fluid contains no $KCl$, $C_{K0} = 0$. Far-field solid composition is $\phi_{K\infty} = 0.3$, $\phi_{Na\infty} = 0.7$. Far-field solid temperature $T_s = 50\,^\circ$C. Three curves plotted, corresponding to far-field fluid temperatures $T_f = -10\,^\circ$C, $T_f = 50\,^\circ$C, and $T_f = 110\,^\circ$C.

dissolution rates of pure $KCl$, both in the régime where salting out of $NaCl$ occurs (solid lines: $\mu$ is leading dissolution front, $\lambda$ is trailing dissolution front), and in the régime where there is a single, planar dissolution front (dashed lines). Dissolution rates are shown as a function of far-field $NaCl$ concentration $C_{Na0}$, for three values of far-field $KCl$ concentration $C_{K0}$.

## 7. Conclusions

We have developed a model for diffusion-and-conduction-controlled, equilibrium dissolution of a homogeneous mixture of two solids A and B ($KCl$ and $NaCl$ being used as the type example), into a ternary solution including materials A and B (water being the type example of the third material). The model admits a solution with two sharp dissolution fronts. The solution has a (central) region occupied partly by aqueous solution, and partly by solid salt B, between a region occupied entirely by aqueous solution, and a region occupied entirely by the original, mixed solid. The leading front can be labelled the salt A dissolution front, and the trailing front the salt B dissolution front.

As long as the solid-B phase equilibrium temperature varies rapidly with the concentration of dissolved salt B, the phase change happens almost entirely at

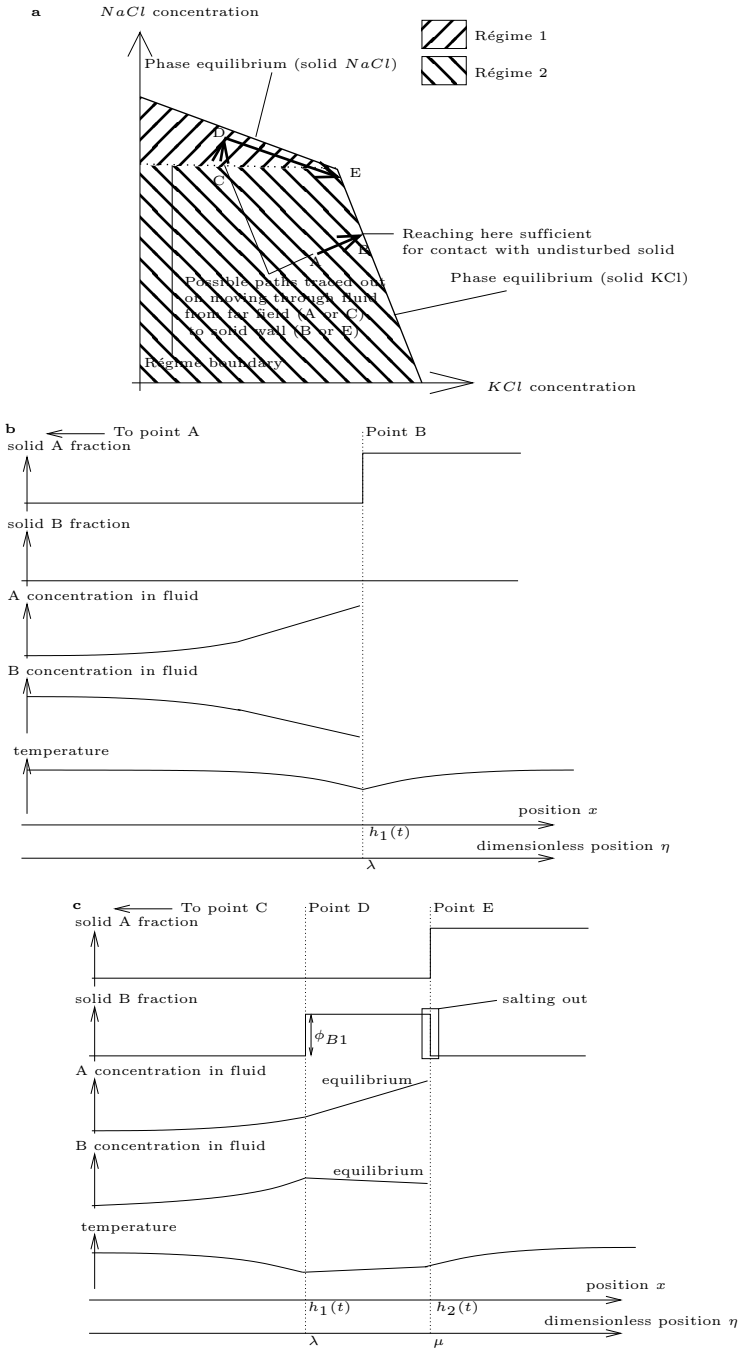


Figure 10. **a:** Schematic of path in (salt A concentration, salt B concentration) space traced out, on moving from far-field fluid (point A) to single front (point B) or from far-field fluid (point C) past trailing front (point D) to leading front (point E), for pure $KCl$ solid, with effect of temperature on phase-equilibrium concentration neglected. **b:** Schematic illustration of solid fractions, concentrations, and temperature, as functions of position, without salting out. **c:** Schematic illustration of solid fractions, concentrations, and temperature, as functions of position, with salting out.

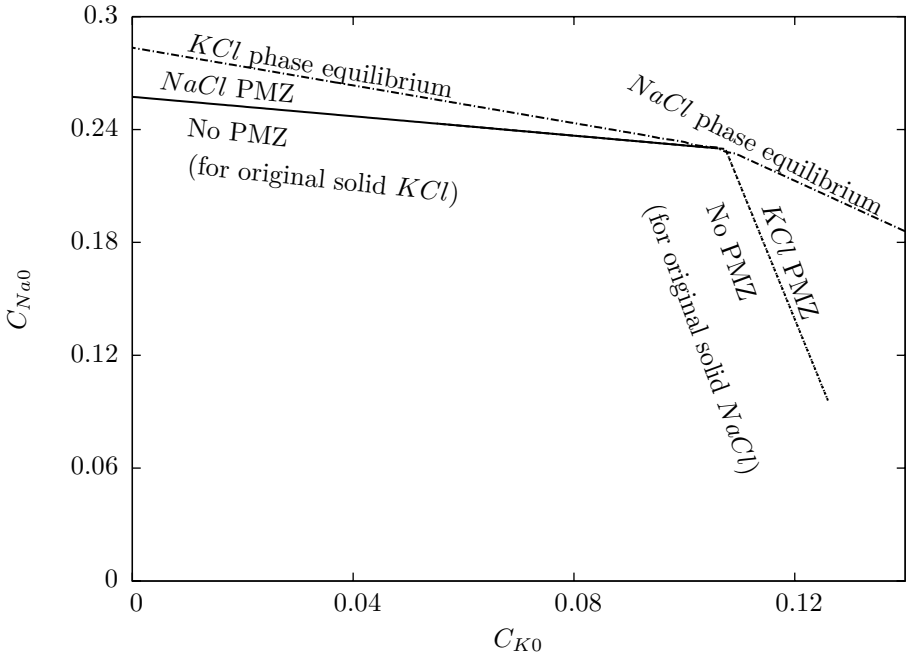


Figure 11. Predicted locus, in (far-field fluid $KCl$ concentration, far-field fluid $NaCl$ concentration) space, of conditions where the two fronts travel together, $\lambda = \mu$, and there is no partially-molten zone. Phase-equilibrium envelope also shown. Far-field solid is pure $KCl$. Far-field fluid temperature $T_f = 50\,^{\circ}\mathrm{C}$. Far-field solid temperature $T_s = 50\,^{\circ}\mathrm{C}$.

the two sharp fronts, and there is almost no distributed phase change within the partially-molten zone.

Some precipitation (of salt B) takes place at the leading front, a phenomenon known (Garrett 1996) as "salting out." However, this may not be the case for other salts, particularly those that have smaller $b_B$, where the effect of the temperature gradient on phase-equilibrium concentration may be sufficient that both salts are transported in the same direction.

There is a unique (for given far-field temperatures) surface in (far-field fluid $KCl$ concentration, far-field fluid $NaCl$ concentration, solid composition) space, dividing conditions under which $NaCl$ is the solid in the partially-molten zone from conditions under which $KCl$ is the solid in the partially-molten zone.

The dissolution rates decrease as the concentration of either salt in the far-field fluid is increased because this reduces the concentration gradients that drive salt transport and therefore dissolution.

In most circumstances, the dissolution front for a given salt moves more slowly as the mass fraction of that salt in the original solid increases. The mass dissolution rates are controlled by the concentration gradients in the fluid and are not strongly affected by the solid composition. This corresponds to a lower dissolution-front speed, as the mass fraction of the dissolving salt in the solid increases.

The dissolution rates increase if either far-field temperature increases, but this effect is smaller than that of concentration. To a good approximation, the tem-

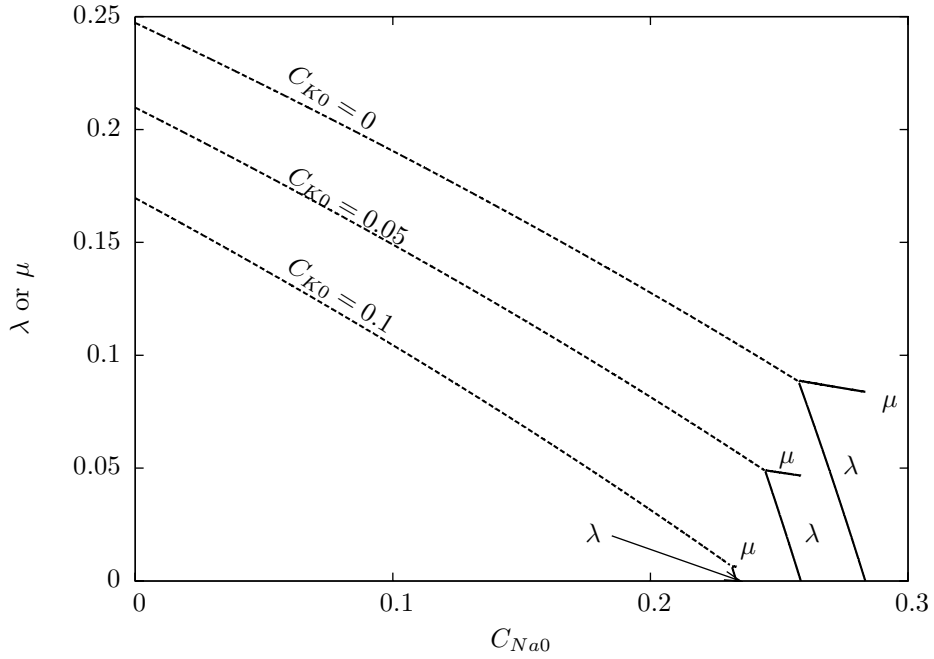


Figure 12. Predicted dimensionless rate constants $\lambda$ and $\mu$, for movement of trailing and leading interfaces, respectively, as functions of $NaCl$ concentration $C_{Na0}$ in far-field fluid. Far-field fluid temperature $T_f = 50\,^\circ$C. Far-field solid is pure $KCl$. Far-field solid temperature $T_s = 50\,^\circ$C. Six curves plotted, corresponding to the two dimensionless rate constants for each of the far-field fluid $KCl$ concentrations $C_{K0} = 0$, $C_{K0} = 0.05$, and $C_{K0} = 0.1$.

perature in and around the partially-molten zone is a weighted average of the two far-field temperatures, although there is a slight suppression due to the need to conduct in heat to supply the latent heat of dissolution. A change in temperature in and around the partially-molten zone produces only a tiny change in concentration, and therefore in the concentration gradients that drive salt transport and dissolution. The lack of salt transport in the solid means that the salt flux (unlike the heat flux) in the liquid adjacent to the interface is a strict control on the dissolution rate. Hence, the small change in salt flux implies a small change in dissolution rate. All the steps in this qualitative physical argument appear to apply also to cases where transport is controlled by buoyancy-driven convection, so one would expect the relative importance of temperature and concentration to be similar in such cases. We are undertaking further study into the details of the dissolution process in the presence of buoyancy-driven convection.

We have also shown that salting out is possible during dissolution of a single-phase solid A by a ternary solution of salts A and B, if the concentration of that solution is sufficiently close to the phase-equilibrium surface of salt B, thereby extending the original model of Hatton & Woods (2007).

The models can be applied directly to solids/solutes other than $KCl$ and $NaCl$, by replacing the parameter values in table 1 with values appropriate to the other solids. However, the analysis relies on the liquidus gradient $b_B$ for the slower-

dissolving solid being large compared with other temperature scales relevant in the partially-molten zone. In particular, this means that, where one of the solids is ice, and the liquid is an aqueous solution of (e.g.) $NaCl$ and $KCl$, the model is valid only as long as ice is the fastest-dissolving of the two solids.

Although the validity of the perturbation expansion requires only the slower-dissolving of the two solids to have a steep liquidus (large $b_B$), the argument for the weak dependence of dissolution rate on far-field temperature relies on the liquidus gradients $a_A$ and $b_B$ for *both* solids being large. Therefore, one would expect the model to predict a greater rôle for temperature if one solid were ice.

## Acknowledgements

We would like to thank Rio Tinto, for financial support.

## References

Arfken, G., 1985 *Mathematical Methods for Physicists*. San Diego: Academic Press, third edn.

Batchelor, G. K., 1973 (1967) *An Introduction to Fluid Dynamics*. Cambridge: Cambridge University Press, first paperback edn.

Carslaw, H. S. & Jaegar, J. C., 1959 (1946) *Conduction of Heat in Solids*. Oxford: Clarendon Press, second edn.

Clauser, C. & Huenges, E., 1995 Thermal conductivity of rocks and minerals. In *Rock Physics and Phase Relations: A Handbook of Physical Constants* (ed. T. J. Ahrens), no. 3 in AGU Reference Shelf, chap. 3-9, pp. 105–126. Washington, DC: American Geophysical Union.

Garrett, D. E., 1996 *Potash: Deposits, Processing, Properties and Uses*. London: Chapman & Hall, first edn.

Glass, D. E., Ozisik, M. N., McRae, S. S. & Kim, W. S., 1991 Formulation and solution of hyperbolic Stefan problem. *J. Appl. Phys.* **70**, 1190–1197. doi:10.1063/1.349572.

Greitzer, E. M., Spakovszky, Z. S. & Waitz, I. A., 2006 *Thermodynamics and Propulsion*. Lecture notes 16, Massachusetts Institute of Technology, Unified Engineering. URL: ⟨`http://web.mit.edu/16.unified/www/FALL/thermodynamics/notes/notes.html`⟩.

Hall, D. L., Sterner, S. M. & Bodnar, R. J., 1988 Freezing point depression of $NaCl$-$KCl$-$H_2O$ solutions. *Econ. Geol.* **83**, 197–202.

Hatton, D. C. & Woods, A. W., 2007 Compositional controls on melting and dissolving a salt into a ternary melt. *Proc. R. Soc. A* **463**, 1211–1229. doi:10.1098/rspa.2007.1819.

Josberger, E. G. & Martin, S., 1981 A laboratory and theoretical study of the boundary layer adjacent to a vertical melting ice wall in salt water. *J. Fluid Mech.* **111**, 439–473. doi:10.1017/S0022112081002450.

Lewis[ Peggs], S. L., 1995 (1911) Densities. In Noyes *et al.* (1995 (1911)), chap. 2.2.1, pp. 41–43. URL: ⟨`http://www.kayelaby.npl.co.uk/general_physics/2_2/2_2_1.html`⟩.

Linke, W. F., 1965 (1907) *Solubilities of Inorganic and Metal-Organic Compounds: A Compilation of Solubility Data from the Periodical Literature*, vol. II: K–Z. Washington, DC: American Chemical Society, fourth edn. A Revision and Continuation of the Compilation Originated by Atherton Seidell, Ph.D., U. S. National Institutes of Health.

MacKay, D. J. C., 2003 *Information Theory, Inference, and Learning Algorithms*. Cambridge: Cambridge University Press. URL: ⟨`http://www.inference.phy.cam.ac.uk/itprnn/book.pdf`⟩.

Marliacy, P., Hubert, N., Schuffenecker, L. & Solimando, R., 1998 Use of Pitzer's model to calculate thermodynamic properties of aqueous electrolyte solutions of $Na_2SO_4 + NaCl$ between 273.15 and 373.15 K. *Fluid Phase Equil.* **148**, 95–106. doi:10.1016/S0378-3812(98)00202-7.

McGlashan, M. L., 1995 (1911)*a* Chemical thermodynamics. In Noyes *et al.* (1995 (1911)), chap. 3.10, pp. 338–357. Originally compiled by G. W. C. Kaye O.B.E., M.A., D.Sc., F.R.S. and T. H. Laby M.A., Sc.D., F.R.S.; now prepared under the direction of an editorial committee. URL: ⟨`http://www.kayelaby.npl.co.uk/`⟩.

McGlashan, M. L., 1995 (1911)*b* Properties of solutions. In Noyes *et al.* (1995 (1911)), chap. 3.6, pp. 266–271. Originally compiled by G. W. C. Kaye O.B.E., M.A., D.Sc., F.R.S. and T. H. Laby M.A., Sc.D., F.R.S.; now prepared under the direction of an editorial committee. URL: ⟨`http://www.kayelaby.npl.co.uk/`⟩.

Morrell, R., 1995 (1911) Thermal conductivities. In Noyes *et al.* (1995 (1911)), chap. 2.3.7, pp. 81–94. URL: ⟨`http://www.kayelaby.npl.co.uk/general_physics/2_3/2_3_7.html`⟩.

Noyes, J. G., Asher, J., Jones, O. C. & Phillips, G. F. (eds.) 1995 (1911) *Kaye & Laby: Tables of Physical and Chemical Constants*. Harlow: Longman, sixteenth edn. Originally compiled by G. W. C. Kaye O.B.E., M.A., D.Sc., F.R.S. and T. H. Laby M.A., Sc.D., F.R.S.; now prepared under the direction of an editorial committee. URL: ⟨`http://www.kayelaby.npl.co.uk/`⟩.

Phillips, G. F., 1995 (1911)*a* Properties of the elements. In Noyes *et al.* (1995 (1911)), chap. 3.1.2, pp. 212–215. URL: ⟨`http://www.kayelaby.npl.co.uk/chemistry/3_1/3_1_2.html`⟩.

Phillips, J. G. E., 1995 (1911)*b* Properties of inorganic compounds. In Noyes *et al.* (1995 (1911)), chap. 3.2, pp. 223–238. URL: ⟨`http://www.kayelaby.npl.co.uk/chemistry/3_2/3_2.html`⟩.

Press, W. H., Teukolsky, S. A., Vetterling, W. T. & Flannery, B. P., 1992 (1986) *Numerical Recipes in Fortran 77: The Art of Scientific Computing*, *Fortran Numerical Recipes*, vol. 1. Cambridge: Cambridge University Press, second edn. URL: ⟨`http://www.nrbook.com/b/bookfpdf.php`⟩.

Ramos, R., Gaisford, S., Buckton, G., Royall, P. G., Yff, B. T. S. & O'Neill, M. A. A., 2005 A comparison of chemical reference materials for solution calorimeters. *Int. J. Pharm.* **299**, 73–83. doi:10.1016/j.ijpharm.2005.04.027.

Richardson, M. J., 1995 (1911) Specific heat capacities. In Noyes *et al.* (1995 (1911)), chap. 2.3.6, pp. 76–81. URL: ⟨`http://www.kayelaby.npl.co.uk/general_physics/2_3/2_3_6.html`⟩.

Sonnenfeld, P., 1985 Occurrence of potash beds within evaporite basins. In *Proceedings of the Symposium Solution Mining of Salts and Brines* (eds. W. J. Schlitt & W. C. Larson), pp. 113–117. Society of Mining Engineers, New York: Society of Mining Engineers.

Titkov, S., 2004 Flotation of water-soluble mineral resources. *Int. J. Miner. Process.* **74**, 107–123. doi:10.1016/j.minpro.2003.09.008.

Vanýsek, P., 2001 Ionic conductivity and diffusion at infinite dilution. In *CRC Handbook of Chemistry and Physics: A Ready-Reference Book of Chemical and Physical Data* (ed. D. R. Lide), pp. 5–95–5–96. Boca Raton: CRC Press, 82nd edn.

Wheeler, D. R. & Newman, J., 2004 Molecular dynamics simulations of multicomponent diffusion: 1. equilibrium method. *J. Phys. Chem. B* **108**, 18353–18361. doi:10.1021/jp047850b.

Woods, A. W., 1992 Melting and dissolving. *J. Fluid Mech.* **239**, 429–448. doi:10.1017/S0022112092004476.